



# Comparison of SEBAL, METRIC, and ALARM algorithms for estimating actual evapotranspiration of wheat crop

Mehdi Asadi<sup>1</sup> · Khalil Valizadeh Kamran<sup>2</sup>

Received: 10 March 2021 / Accepted: 19 March 2022 / Published online: 18 April 2022  
© The Author(s), under exclusive licence to Springer-Verlag GmbH Austria, part of Springer Nature 2022

## Abstract

Evapotranspiration is one of the main components of water balance and its accurate estimation is of great importance in planning and optimizing water consumption. In this study, therefore, it was tried to calculate the actual evapotranspiration rate of wheat crop in the Pars Abad section of Moghan plain, northwestern Iran, which is one of the main agricultural hubs in Iran. The research tools were Surface Energy Balance Algorithm for Land (SEBAL), Mapping Evapotranspiration at High Resolution with Internalized Calibration (METRIC), and Analytical Land Atmosphere Radiometer Model (ALARM) methods. For this purpose, 12 images of Landsat 7 and 8 satellites were used, all of which were in the product development period between 2016 and 2019, and the results were compared with lysimeter data. The results indicated that the highest actual evapotranspiration rate of wheat crop during the development period was related to 2018.07.01 (7.86 mm/day) in the ALARM method and the lowest rate in the mid-growth period belonged to 2017.01.30 (0.32 mm/day) in the METRIC method. Among the investigated methods, the SEBAL method with an RSME of 0.633 had the lowest error rate and the highest  $R^2$  (0.9307) compared with the lysimeter data, followed by the METRIC and ALARM methods with the lowest error (RMSE = 0.761 and 0.855 mm/day) and the highest correlation ( $R^2 = 0.9057$  and 0.8709), respectively.

## 1 Introduction

Evapotranspiration is one of the main components of water balance in any region and also one of the key factors for proper planning of irrigation to improve water use efficiency in agricultural lands (Li et al. 2008). Since, the Moghan plain is one of the principal centers of agriculture and wheat production in Iran. The arable land in this plain is about 320 thousand hectares, of which only 30 thousand hectares are irrigated in a modern way. Therefore, in the current situation, the main problem of farmers in most areas of Moghan plain is not the lack of water, but the main problem is how to manage and use water resources. Because the irrigation efficiency in the developed countries of the world is more than 90%, but in the best condition, the irrigation efficiency of agricultural lands in Moghan plain is only 25% (Nasrabadi 2015). So by using

the results of the present study, by spending less time and cost, while determining the exact amount of actual evapotranspiration of wheat crop in the study area, wastage of water can be prevented, and irrigation efficiency can be increased. Due to lack of awareness of the water needs of plants in the region, especially wheat has caused farmers to use incorrect irrigation methods in wheat cultivation and cause a lot of wastage of water and practically cause pressure on the surface and subsurface water in the region. Therefore, due to the centrality of the Moghan plain in the agricultural sector, especially in wheat production, it can cause irreparable damage to food security in the future. Various methods have been developed to evaluate evapotranspiration in different land use and environmental conditions using meteorological data. However, most of these methods (lysimeter, eddy covariance, etc.) use local fixed data that is only appropriate at the local scale (Liou and Kar 2014; Kundu et al. 2018) and also have staggering costs (Ruhoff et al. 2012; Horvat 2013; Ata-sever and Ozkan 2018). In this study, therefore, it was tried to measure the evapotranspiration rate using satellite imagery and remote sensing algorithms. In the recent decades, there has been increasing use of these images and methods to estimate evapotranspiration rates. This is

✉ Mehdi Asadi  
Asadimehdi11@yahoo.com

<sup>1</sup> Agricultural Climatology, Hakim Sabzevari University, Sabzevar, Iran

<sup>2</sup> Department of Remote Sensing and GIS, University of Tabriz, Tabriz, Iran

because these methods can estimate the evapotranspiration rate regardless of soil conditions, crop, and farm management (Moradi et al. 2020).

Many types of research have been done to estimate the actual evapotranspiration of crops employing the remote sensing algorithms, of which a few cases are mentioned here. Suleiman et al. (2008) evaluated evapotranspiration of the wheat at Different Ecological Zones in Jordan by using the ALARM method. The results showed that the amounts of evapotranspiration of wheat from site to site have significant differences. Reasons for this variability include soil types, vegetation cover, irrigation, and warm advection. Lian and Huang (2015) evaluated evapotranspiration of spring wheat for an Oasis Area in the Heihe River Basin using Landsat-8 images and the METRIC Model. The results showed that METRIC can provide reasonable ET estimates in the heterogeneous land use types under advective environmental conditions with the selection of appropriate extreme pixels. Rawat et al. (2017) determined the evapotranspiration rate of wheat crop and created maps using SEBAL algorithm in Bhiwani Haryana Area, India, and compared the results with the FAO Penman–Monteith method and lysimeter. The results manifested that evapotranspiration from SEBAL model was correlated ( $r^2$ ) with those of lysimeter and FAO Penman–Monteith with values of 0.91 and 0.85, respectively. French et al. (2018) utilized METRIC method and Landsat images to evaluate the evapotranspiration of wheat over the Central Arizona Irrigation and Drainage District, USA. Results revealed that remote sensing of actual ET could lead to significantly improved estimates of crop water use. Rahimzadegan and Janani (2019) estimated the evapotranspiration rate of pistachio crop using SEBAL algorithm and Landsat 8 satellite imagery and compared the results with the Intelligent Meteorological Instrument (iMetos-Pessl). They obtained  $r^2$  and RMSE of 0.8 and 2.5 mm/day, respectively. Khand et al. (2021) evaluated modeling evapotranspiration of winter wheat using Contextual and Pixel-Based Surface Energy Balance Models (SEBAL, METRIC, and SEBS). Results showed that the METRIC model's RMSE (0.14 mm/day) was smaller than the SEBAL and SEBS methods. From the examination of the researches carried out in Iran and the study area, it has been observed that most of the studies have estimated the rate of evapotranspiration in a specific region (Jovzi et al. 2019; Zoratipour et al., 2019; Asadi and Karami 2020) and very little research has been done on the water requirements of the products. In other words, a kind of vacuum has been created in this field. Therefore, in addition to investigation of evapotranspiration in the study area, the authors in this study have tried to investigate the water requirement of wheat crops using SEBAL, METRIC, and ALARM remote sensing methods. Then compare the results with the data obtained from the lysimeter, which was unprecedented in the whole study

area and Iran before this study and can be considered as a research innovation.

The main purpose of this research was to estimate the actual evapotranspiration rate of wheat crop (one of the main and dominant crops in the region) using different remote sensing methods (SEBAL, METRIC, and ALARM) in the Pars Abad section of Moghan plain as one of the main agricultural hubs in northwestern Iran. Finally, the results were compared with those of lysimeter data.

## 2 Materials and methods

### 2.1 Study area

The Moghan Plain is located in 38.44°–39.42° N and 47.9°–48.22° E, in the north of Ardabil province in Iran (Fig. 1). The mentioned plain, due to its agricultural prosperity, is one of the principal agricultural hubs of Iran, with extensive and blockaded farmlands, and an area under wheat cultivation of approximately 29,200 hectares. A large block of this area (432 hectares, between 39.36°–39.38° N and 47.55°–47.57° E. The lysimeter is located in 39° 38' 33 N–47° 56' 13 E) was selected (Fig. 1) to estimate the actual evapotranspiration value (The selected block is operated under the supervision of Moghan Agro-Industry and Livestock Company, which has irrigation management and its agriculture is well controlled as well as the soil conditions do not restrict proper plant growth). The average elevation of the plain is 42 m above sea level, and the average rainfall and temperature are 308.9 mm and 14.94 °C, respectively; accordingly, it falls in the Mediterranean climate category based on the De Martonne classification.

### 2.2 Research data

#### 2.2.1 Meteorological data

Landsat 7 and Landsat 8 satellite images (OLI and TIRS sensors) for row 33 and path 167 include visible bands, near infrared, and thermal infrared.

Daily and 3-h statistics of synoptic stations in the northern half of Ardabil province including average daily and 3-h temperature, minimum temperature, maximum temperature, sunny hours, wind speed, daily data of class A evaporation pan, relative humidity, and related data about the cultivation time of the examined crops.

Information extracted from the image help file: This file, known as the header file, contains very important information for use in various stages of execution of SEBAL, METRIC, and ALARM algorithms and includes the time and date of imaging of the study area, the angle of the

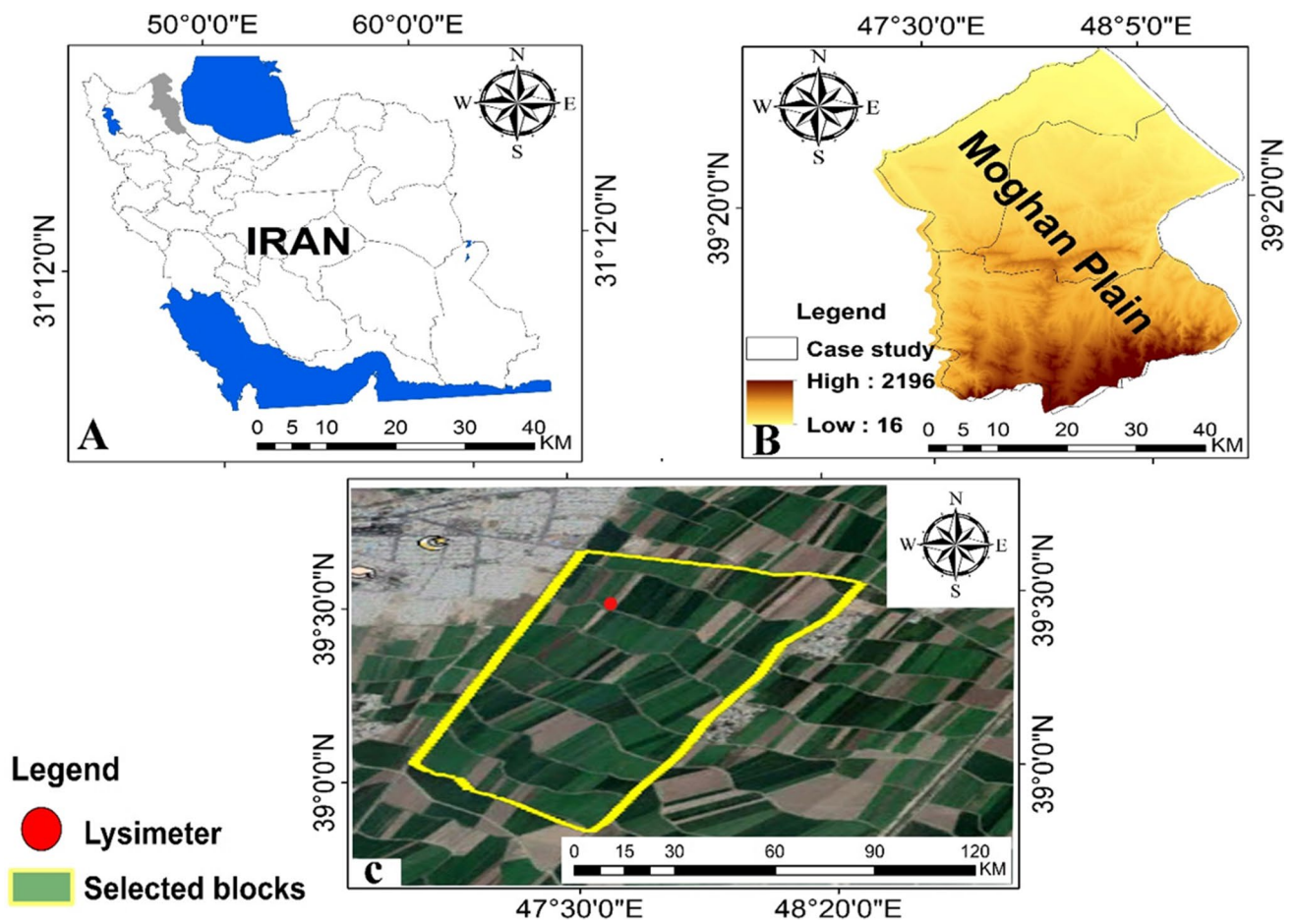


**Fig. 1** The study area. **A** The relative position of Moghan plain in Iran. **B** Moghan plain. **C** Selected blocks from fields under wheat cultivation and Lysimeter is also located in this area

solar azimuth, solar elevation angle, calibration coefficients for conversions related to spectral radiance and reflectance, and distance from the sun to the ground.

interference (SLC-Off image) (Widyantara and Solihuddin 2020; Alexandridis et al. 2013). The specifications of the images used are shown in Table 1.

**2.2.2 Satellite images**

In this study, Landsat 8 cloudless images during wheat crop growth period (from 9 October to 14 July) from 2016 to 2019 (for the study area) were used to estimate actual evapotranspiration of wheat crop. The Landsat 7 images were also used here since there was no access to Landsat 8 cloudless images at certain stages of the crop development period. As Landsat 7 images have errors since 2003, gapfill extension and triangulation method were used to fix the errors. Gapfill correction was carried out to overcome Scan Line Corrector (SLC) in Landsat images using Landsat gapfill tools processing type single file gapfill (triangulation). This type of processing does not require a fill image (SLC-On image) to fill in the gaps in the image experiencing stripping

**Table 1** Landsat images used during wheat crop cultivation

No	Year	Date	Satellite	Growth stage
1	2019	26 FEB	Landsat 8	Mid
2	2019	1 MAY	Landsat 8	Mid
3	2019	17 JUN	Landsat 8	Development
4	2018	12 APR	Landsat 8	Mid
5	2018	22 MAY	Landsat 7	Mid
6	2018	1 JUL	Landsat 8	Development
7	2018	21 OCT	Landsat 8	Initial
8	2017	30 JAN	Landsat 8	Mid
9	2017	11 MAY	Landsat 8	Mid
10	2017	27 JUN	Landsat 8	Development
11	2017	17 OCT	Landsat 8	Initial
12	2016	7 OCT	Landsat 7	Initial

It should be noted that since all the images used were downloaded from <https://earthexplorer.usgs.gov/>, these images are free of any geometric errors and only require radiometric corrections including the physical components reflectance and radiance and SLC error of Landsat 7 (for further information see Allen et al. 2002).

### 2.3 Surface Energy Balance Algorithm

Energy equilibrium algorithms such as SEBAL, METRIC, and ALARM are methods that estimate the instantaneous and daily evapotranspiration values of a crop based on physical and experimental relationships using satellite imagery and low-ground observational data (Bastiaanssen et al. 1998; Su 2002; Owaneh and Suleiman 2018). To estimate evapotranspiration using the SEBAL, METRIC, and ALARM methods, first the mathematical relationships were identified needed to perform analysis such as reflectance, vegetation index, emissivity, surface albedo, surface temperature, net radiations, soil heat flux, sensible heat flux, latent heat flux. Finally, calculations were made for the instantaneous flux and the amount of daily evapotranspiration, as described below.

The mentioned methods are significantly dependent on the thermodynamic energy balance between processes occurring on the Earth surface and the atmosphere which is called surface energy balance. Ultimately, this method obtains the latent heat flux to estimate the actual daily evapotranspiration value by establishment of energy balance between the surface and the atmospheric phenomena, expressed by Eq. (1) (Mkhwanazi et al. 2015).

$$LE = Q^* - G - H \quad (1)$$

where  $LE$  is the latent heat flux ( $W/m^2$ ),  $Q^*$  is the net radiations ( $W/m^2$ ),  $G$  is the soil heat flux ( $W/m^2$ ), and  $H$  is the sensible heat flux ( $W/m^2$ ).

The net radiation flux ( $Q^*$ ) is the amount of radiation at the surface expressed by the difference between the incoming and outgoing radiation from Eq. (2).

$$Q^* = (1 - r_0) \cdot K \downarrow - L \downarrow - L \uparrow - (1 - \epsilon_0) \cdot L \downarrow \quad (2)$$

where  $K \downarrow$  is the incoming shortwave radiation ( $W/m^2$ ),  $L \downarrow$  is the incoming longwave radiation ( $W/m^2$ ),  $L \uparrow$  is the outgoing longwave radiation ( $W/m^2$ ),  $r_0$  is the surface albedo, and  $\epsilon_0$  is the surface emissivity (for further information have a look at Allen et al. 2002).

The METRIC and ALARM methods are similar to the energy balance equation based on the SEBAL method (Eq. 1). Therefore, in order to avoid repetition, only the

equations that differ in all three methods will be discussed below.

The METRIC model, except in a few cases, is also used to obtain the net radiation flux from the same SEBAL model relation and both methods use hot and cold pixels to calculate the sensible heat flux. In the SEBAL model, only the mean sea level is used to calculate transmissivity, whereas in addition to the amount of atmospheric pressure in the metric method, the amount of water entering the atmosphere is also calculated by Eq. (3) (Allen et al. 2007):

$$\tau_{sw} = 0.35 + 0.627 \times \exp \left[ \frac{-0.00146p}{K_t \cos \theta_{hor}} - 0.75 \left( \frac{w}{\cos \theta_{hor}} \right)^{0.4} \right] \quad (3)$$

where  $p$  is the atmospheric pressure (kPa),  $K_t$  is the unitless turbidity coefficient  $0 < K_t \leq 1.0$  where  $K_t$  is 1.0 for clean air and 0.5 for extremely turbid, dusty, or polluted air,  $\theta_{hor}$  is the solar zenith angle over a horizontal surface, and  $w$  is the water in the atmosphere (mm).

The parameters  $p$  and  $w$  are calculated through Eqs. 4 and 5 (Losgedaragh and Rahimzadegan 2018):

$$p = 101.3 \left( \frac{293 - 0.0065z}{293} \right)^{5.26} \quad (4)$$

$$w = 0.14 e_a P_{air} + 2.1 \quad (5)$$

where  $z$  is the elevation above sea level (m),  $e_a$  is near-surface vapor pressure (kPa), and  $P_{air}$  is air pressure (kPa).

Soil heat flux ( $G$ ) is mainly driven by very dynamic thermal gradients in time and space in surface soil (Singh et al. 2008). Various studies have shown that soil heat flux can be calculated as far albedo, biomass, and surface temperature as a fraction of net radiation (Daughtry et al. 1990; Kustas and Daughtry 1990; Kustas et al. 1994; Bastiaanssen 1998; Bastiaanssen 2000; Jacob et al. 2002). The mathematical form of it is expressed in Eq. (6):

$$\frac{G}{Q^*} = T_s - 237.15/r_0 \cdot \{0.0038 \cdot r_0 + 0.007 \cdot r_0^2\} \cdot \{1 - 0.98 \cdot (NDVI^4)\} \quad (6)$$

where  $\frac{G}{Q^*}$  is the fraction of net radiation flux and soil heat flux,  $T_s$  is the surface temperature ( $^{\circ}C$ ), and NDVI is the normalized difference vegetation index.

Sensible heat flux ( $H$ ) is the amount of heat lost to the air by convection and conduction or the surrounding environment due to temperature gradient (Allen et al. 2005; Oberg and Meless 2006). Sensible heat flux calculations are the most difficult part of the SEBAL algorithm because of two unknowns (temperature difference and aerodynamic resistance to heat transport) and are estimated from Eq. (7) (Costa et al. 2019):



$$H = \rho \cdot C_p \cdot \left( \frac{a + (b * Ts)}{rah} \right) \tag{7}$$

where  $\rho$  is the air density ( $\text{kg/m}^3$ ),  $C_p$  is the air specific heat ( $1400\text{J/kg/K}$ ),  $a + b$  are the experimental coefficients determined through an internal calibration for each satellite image. This part is determined by the choice of hot (dry pixels) and cold (wet pixels) pixels and is very sensitive because it directly affects the calculation results related to the sensible heat flux and the evapotranspiration rate.  $rah$  is the aerodynamic resistance to heat transport. According to the SEBAL method, the aerodynamic resistance of the temperature transfer must first be calculated with stability atmospheric conditions to calculate the initial value of the sensible heat flux and then, the correction heat flux values are calculated for all pixels by calculating the Monin–Obukhov length ( $L$ ) and iterations of the calculation process. Thus, the frictional velocity ( $u^*$ ) is calculated from Eq. (8):

$$u^* = u_{200} \times 0.41 \sqrt{\ln\left(\frac{200}{z_{0m}}\right) - \Psi_{m(200m)}} \tag{8}$$

Finally, the aerodynamic resistance to heat transfer is calculated by Eq. (9):

$$r_{ah} = \ln\left(\frac{z_2}{z_1}\right) - \Psi_{h(z_2)} + \Psi_{h(z_1)}/u^* \times 0.41 \tag{9}$$

where  $\Psi_{m(200m)}$  is the stability correction for momentum transport at 200 m,  $\Psi_{h(z_1)}$  is the stability correction for heat transport at 1 m, and  $\Psi_{h(z_2)}$  is the stability correction for heat transport at 2 m (for further information refers to Allen et al. 2002).

The ALARM model uses the same relationships as the SEBAL and METRIC methods to calculate net radiation flux and soil heat flux. However, the ALARM model uses a different approach based on the Monin–Obukhov similarity theory (MOS) to calculate sensible heat flux values as opposed to the SEBAL and METRIC models and does not consider hot and cold pixels. In fact, the main difference between these models is the estimation of the surface temperature and the coefficient of roughness length for the sensible heat. According to ALARM, the direct use of land surface temperature is not useful for estimating the amount of sensible heat flux for vegetation because the radiometric surface temperature calculated from satellite images is different from the temperature required to cover the plant canopy, known as the aerodynamic surface temperature ( $T_i$ ). Therefore, the direct use of land surface temperature can have significant errors in estimating the sensible heat flux. In addition, to find precise values of  $H$ , we need to find precise values of  $Z_{oh}$ , which is dependent on the surface temperature profile of the atmospheric layer (Eq. 10). Since the exact surface temperature profiles are not well defined for vegetation,

it is therefore not easy to determine the correct values of  $Z_{oh}$ . These methods use two separate approaches to solve this problem in which SEBAL and METRIC remove the aerodynamic temperature ( $T_i$ ) value from the calculation process; hence, there is no need to specify  $Z_{oh}$  values; it uses two dry and wet pixels to obtain the value of  $H$  assuming a linear relationship between  $dt$  and land surface temperature. In contrast, ALARM has developed an approach that predicts the values of  $T_i$  and  $Z_{oh}$ . ALARM converts the value of  $T_s$  to  $T_i$  by modifying the vegetation temperature profile and, by considering the leaf area index (LAI), canopy height, leaf angle distribution, and sensor zenith view angle are obtained by  $Z_{oh}$ , Eq. (12) (see the following resources for more information: Suleiman and Crago 2002a, b; Suleiman et al. 2007; Suleiman and Al-Bakri 2011; Owaneh and Suleiman 2018).

$$H = \frac{(T_s - T_a)ku_*\rho c_p}{\left[ \ln\left(\frac{z_a - d_o}{z_{oh}}\right) - \varphi\left(\frac{z_a - d_o}{L}\right) \right]} \tag{10}$$

where  $T_a$  is the air temperature at  $z_a$  in the surface sublayer,  $z_{oh}$  is the scalar roughness length for sensible heat, and  $d_o$  is the displacement height (Suleiman et al. 2008).

### 2.3.1 Calculations of the 24-h evapotranspiration based on SEBAL, METRIC, and ALARM methods

In the SEBAL and METRIC methods to obtain the amount of daily evapotranspiration, first, the instantaneous evapotranspiration flux is calculated and this parameter is the instantaneous evapotranspiration values versus evapotranspiration depth, and is calculated from the relation 11 (Genanu et al. 2017):

$$ET_{inst} = 3600 \times \frac{\lambda ET}{\lambda} \tag{11}$$

where  $ET_{inst}$  is the instantaneous evapotranspiration (mm/h), and 3600 is used to convert seconds to hours.

But obtaining the daily evapotranspiration is usually more useful than having instantaneous evapotranspiration because most of the planning is done thereon. Therefore, it is used to calculate daily evapotranspiration by multiplying the reference evapotranspiration by a 24-h total evapotranspiration reference based on Eq. (12) (AlZayed et al., 2016):

$$ET_{24} = ET_r F \times ET_{r-24} \tag{12}$$

where  $ET_{r-24}$  is the cumulative 24-h  $ET_r$  for the day of the image, and  $ET_r F$  is the reference ET fraction.

In the ALARM method, after obtaining net radiation flux, soil heat flux, and finally no dimensional temperature changes, the amount of latent heat flux into the atmosphere can be calculated from Eq. (13). The evaporation fraction

amount is estimated using Eq. (14), and the actual evapotranspiration value is calculated by placing it in Eq. (15) (Suleiman and Crago 2004).

$$E = (R_n - G)(1 - \Delta_T) \quad (13)$$

$$EF = \frac{E}{(R_n - G)} = 1 - \Delta_T = \frac{T_{\max} - T_i}{T_{\max} - T_a} \quad (14)$$

$$ET = \left( \frac{EF * 3600}{\lambda} \right) * 1000 \quad (15)$$

## 2.4 Validation

In this study,  $R^2$  and RMSE were used to evaluate the performance of SEBAL, METRIC, and ALARM methods against lysimeter data for estimation of water requirement of wheat crop in Pars Abad of Moghan plain (Lysimeter data was obtained from the Ardabil Meteorological Organization). The lysimeter used in this study is a non-weighted drainage lysimeter. The desired lysimeter has a diameter of 2 m and a depth of 1.5 m. The slope of the lysimeter floor is about 7%. The soil in lysimeters (sandy loam) is the same as the soil around the lysimeter. Irrigation is done twice a week, at 8 o'clock on Sunday and 16 o'clock on Wednesday. Also, twice a day at 10 and 18 o'clock, drained water, if any, was measured. Relationships related to these statistics are as follows (Zhou et al. 2014):

$$RMSE = \sqrt{\frac{\sum_{i=1}^n (E_{si} - E_{oi})^2}{n}} \times 100 \quad (16)$$

$$R^2 = \frac{\left( \sum_{i=1}^n (E_{si} - \bar{E}) \right) \left( E_{oi} - \bar{E}_{oi} \right)}{\left( \sum_{i=1}^n (E_{si} - \bar{E}) \right)^2 \left( E_{oi} - \bar{E}_{oi} \right)^2} \quad (17)$$

where the  $E_{si}$ ,  $E_{oi}$ , and  $\bar{E}$  values are related to evapotranspiration estimated by lysimeter and SEBAL, METRIC, and ALARM methods and mean values, respectively.

## 3 Results and discussions

### 3.1 Evapotranspiration distribution map in the study area

According to the definition, the SEBAL, METRIC, and ALARM methods obtain the latent heat flux to estimate the actual daily evapotranspiration value (Table 2) by balancing the energy between the surface and atmospheric phenomena

**Table 2** Actual evapotranspiration in the study area

No	Date	SEBAL (mm/day)	METRIC (mm/day)	ALARM (mm/day)
1	26/02/2019	2.38	2.84	2.48
2	01/05/2019	10.59	10.65	10.71
3	17/06/2019	11.02	10.94	11.22
4	12/04/2018	5.85	6.08	6.40
5	22/05/2018	9.85	9.63	10.37
6	01/07/2018	12.54	12.11	13.46
7	21/10/2018	4.70	4.07	5.24
8	30/01/2017	1.32	1.50	2.01
9	11/05/2017	10.58	9.64	10.68
10	27/06/2017	11.41	11.24	11.86
11	17/10/2017	4.32	4.68	5.01
12	07/10/2016	4.96	4.80	5.45

(net radiation flux, soil heat flux, and sensible heat flux). Table 2 shows the actual evapotranspiration in the study area based on the studied methods. The highest true evapotranspiration rate is related to date 2018.07.01 in all three SEBAL, METRIC, and ALARM methods with values of 12.54, 12.11, and 13.46 mm/day, respectively, in the whole region. In contrast, the lowest actual evapotranspiration rate in the whole region is related to date 2017.01.30 with values of 1.32, 1.50, and 2.01 mm/day in all three SEBAL, METRIC, and ALARM methods, respectively, which seems normal given their location in July and January (the hottest month and the coldest month in the region, respectively). Figures 2 and 3 show the minimum and maximum values of actual evapotranspiration in the study area based on the SEBAL, METRIC, and ALARM methods, respectively, the northern regions of the study area have more actual evapotranspiration than the southern ones because the former has high vegetation and moisture content than the latter area. Therefore, it can be concluded that the amount of evapotranspiration in each region is a reflection of the climatic conditions of that region and is affected by some climatic parameters such as sunshine hours, temperature, wind speed, and humidity, which directly affected the optimal conditions of the crop growth. Hence, by estimating the rate of evapotranspiration, the farmer not only can harvest the product with higher quality but also can manage the water resources.

### 3.2 Evapotranspiration of wheat crop based on SEBAL, METRIC, and ALARM methods

After performing the required calculations of the SEBAL, METRIC, and ALARM algorithms and providing actual evapotranspiration maps throughout the study area, the actual evapotranspiration maps of wheat crop were plotted in the selected block (Fig. 4). The actual

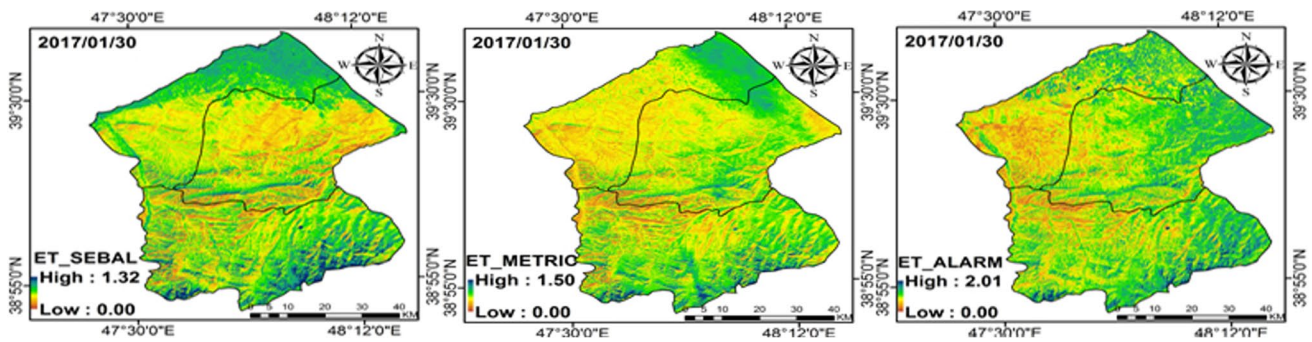


**Fig. 2** The minimum values of actual evapotranspiration in the study area based on SEBAL, METRIC, and ALARM methods

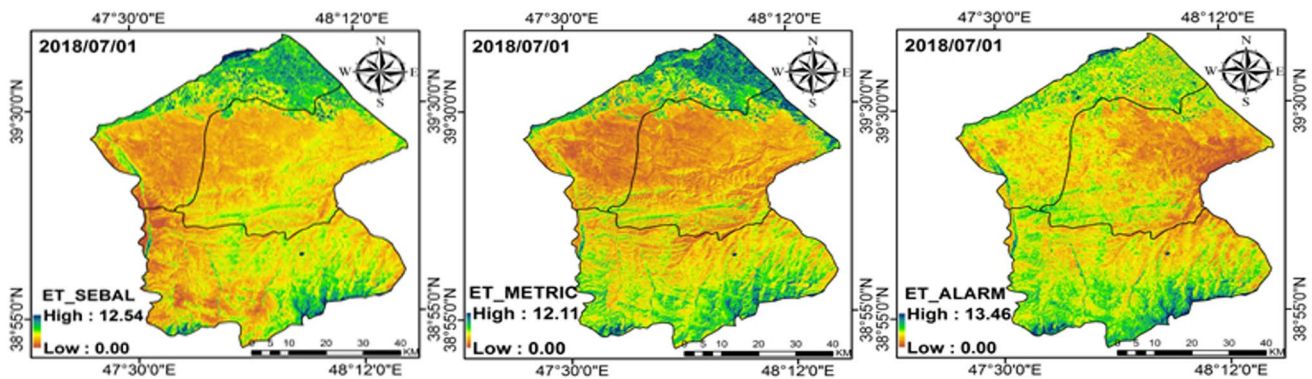


**Fig. 3** The maximum values of actual evapotranspiration in the study area based on SEBAL, METRIC, and ALARM methods

evapotranspiration values were obtained for each of the methods studied in different cultivation periods of the plant (Table 3). According to Table 3, the highest actual evapotranspiration rate of wheat crop during the initial growth period occurs on 2018.10.21 in SEBAL (3.01 mm/day), METRIC (2.95 mm/day), and ALARM (3.23 mm/day) methods, respectively, and the lowest values in the above methods with values of 1.31, 1.19, and 1.64 mm/day are related to the dates 2016.10.07 (SEBAL and ALARM) and 2017.10.17 (METRIC), respectively. Also, the highest actual evapotranspiration rate of wheat crop in mid-growth period is related to date 2017.05.11 in SEBAL (4.63 mm/day), METRIC (4.54 mm/day), and ALARM (4.80 mm/day) methods, respectively, and the lowest value in the above methods with values of 0.49, 0.32, and 0.77 mm/day belongs to date 2017.01.30, respectively. Finally, the highest actual evapotranspiration rate of wheat crop during the develop-growth period is related to date 2018.07.01 in SEBAL (7.42 mm/day), METRIC (7.54 mm/day), and ALARM (7.86 mm/day) methods respectively, and the lowest values in the above methods with values of 7.06, 6.14, and 5.74 mm/day are related to the dates 2019.6.17 (SEBAL) and 2017.6.27 (METRIC and ALARM).

Then, the results of these methods (SEBAL, METRIC, and ALARM) were compared with lysimeter data (Table 3), in which, based on the lysimeter data the highest evapotranspiration rate (8.1 mm/day) in the develop-growth period is related to date 2018.07.01 and the lowest evapotranspiration rate (0.91 mm/day) in the mid-growth period belongs to date 2017.01.30.

### 3.3 Validation

Among the investigated methods, SEBAL has the lowest RMSE (0.633 mm/day) and  $R^2$  (0.9307) with lysimeter data, followed by the METRIC and ALARM methods with RMSE values of 0.761 and 0.855 mm/day and the  $R^2$  values of 0.9057 and 0.8709, respectively, in terms of the least error and the highest correlation (Table 4).

A review of the literature revealed that the results of the present study are highly consistent with some previous research works. Mkhwanazi et al. (2015) estimated water requirements of beans, wheat, and maize crops using the SEBAL and SEBAL A methods and compared their RMSE values between beans and wheat using the SEBAL A (0.82 mm/day) and SEBAL (1.97 mm/day) methods. Ma



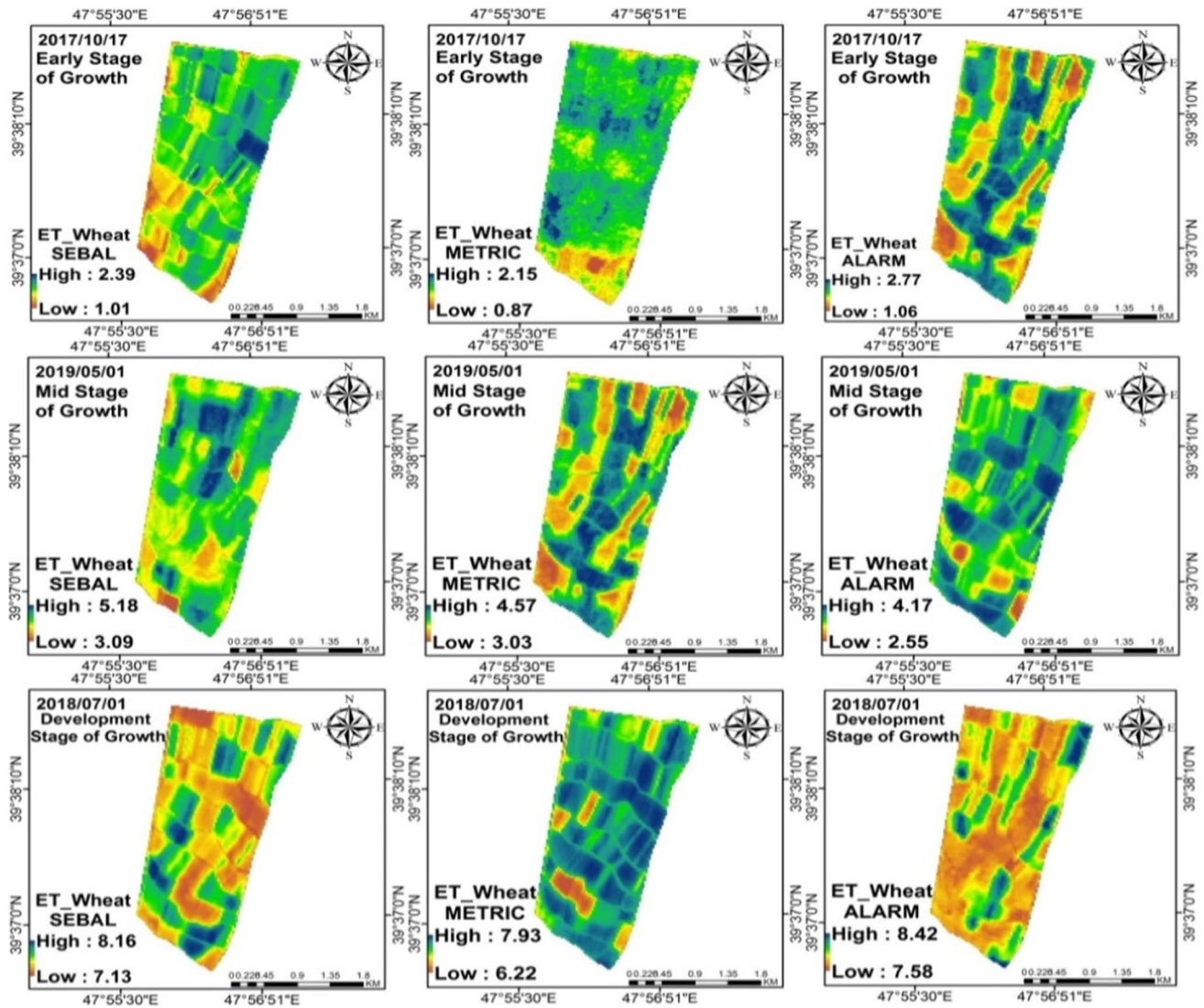


**Fig. 4** Actual evapotranspiration values of wheat crop in the studied block in selected crop growth periods based on SEBAL, METRIC, and ALARM methods

**Table 3** Actual evapotranspiration of wheat crop in the selected block based on the studied methods

No	Date	Growth stage	Lysimeter (mm/day)	SEBAL (mm/day)	METRIC (mm/day)	ALARM (mm/day)
1	26/02/2019	Mid	1.03	0.67	0.64	0.97
2	01/05/2019	Mid	3	3.64	3.58	3.6
3	17/06/2019	Develop	7.25	7.06	6.97	6.45
4	12/04/2018	Mid	3.45	4.21	4.02	4.54
5	22/05/2018	Mid	3.9	4.08	3.84	4.18
6	01/07/2018	Develop	8.01	7.42	7.54	7.86
7	21/10/2018	Initial	3.24	3.01	2.95	3.23
8	30/01/2017	Mid	0.91	0.49	0.32	0.77
9	11/05/2017	Mid	3.11	4.63	4.54	4.80
10	27/06/2017	Develop	7.58	7.34	6.14	5.74
11	17/10/2017	Initial	2.12	1.77	1.19	1.93
12	07/10/2016	Initial	2.06	1.31	1.42	1.64



**Table 4** Comparison of lysimeter values with remote sensing methods in terms of RMSE (mm/day) and  $R^2$ 

	SEBAL	METRIC	ALARM
RMSE mm/day	0.633	0.761	0.855
$R^2$	0.9307	0.9057	0.8709

et al. (2012) estimated water requirements of such crops as wheat and rice and measured an RMSE value of 0.74 mm/day using SEBS algorithm and Landsat 5 satellite imagery. Ma et al. (2013) estimated the water requirement of crops such as wheat, barley, and maize relative to ground data with an RMSE of 0.89 mm/day using SEBS and ASTER satellite imagery. Elnmer et al. (2019) estimated the daily and seasonal evapotranspiration of crops (e.g., wheat) in the Nile Delta using SEBAL method in comparison to the Penman–Monteith method, and estimated an RMSE value of 0.465 mm/day between these methods. Rahimpour and Rahimzadegan (2021) evaluated surface energy balance algorithm for land and operational simplified surface energy balance algorithm over freshwater and saline water bodies in Urmia Lake Basin. The results showed the root mean square error for SEBAL result ( $RMSE_{SEBAL}$ ) as 2.0 mm/day, the correlation coefficient ( $R_{SEBAL}$ ) as 0.80 mm/day, and  $RMSE_{SSEBop}$  and  $R_{SSEBop}$  as 1.7 and 0.80 mm/day, respectively. Examining the researches done especially in Iran, it was found that most of the researchers have estimated the amount of evapotranspiration in a region based on the reference plant or by one method. In contrast, the actual amount of evapotranspiration or water requirement of the crops has not been done. Therefore, the main purpose of this study is to investigate the evapotranspiration in the region and to investigate the water requirement of the wheat crop in the region using remote sensing methods such as SEBAL, METRIC, ALARM and compare the results with the Lysimeter data. Finally, the accuracy of remote sensing methods such as SEBAL, METRIC, and ALARM in comparison with the lysimeter data in estimating the water requirement of the wheat crop was evaluated in arid and semi-arid regions such as Iran. It should be noted that the ALARM method has been studied for the first time in Iran.

## 4 Conclusions

In the present study, the actual evapotranspiration values of wheat crop were obtained at different growth periods in Pars Abad of Moghan plain using remote sensing methods and the results were compared with the lysimeter data from the Ardabil Meteorological Organization. The results showed the highest actual evapotranspiration rates of wheat crop in SEBAL (3.01 mm/day), METRIC, (2.95 mm/day), and

ALARM (3.23 mm/day) methods during the initial growth period on 2018.10.21. Also, the highest actual evapotranspiration rate of wheat crop in mid-growth period was recorded on 2017.05.11 in SEBAL (4.63 mm/day), METRIC (4.54 mm/day), and ALARM (4.80 mm/day) methods. Finally, the highest actual evapotranspiration rate of wheat crop during develop-growth period belonged to date 2018.07.01 in SEBAL (7.42 mm/day), METRIC (7.54 mm/day), and ALARM (7.86 mm/day) methods. Among investigated methods, SEBAL has the lowest RMSE (0.633 mm/day) and the highest  $R^2$  (0.9307) with lysimeter data. Then the METRIC and ALARM methods with RMSE values of 0.761 and 0.855 mm/day and  $R^2$  values of 0.9057 and 0.8709, respectively, have the least error and the highest correlation with lysimeter data. Based on the results obtained, using the SEBAL, METRIC, and ALARM remote sensing methods and the minimal use of ground data in the present study, the water requirement of essential crops, such as wheat and barley, can be estimated with reasonable accuracy. As a result, it is possible to make maximum use of water resources by reforming the cultivation and irrigation management of crops and with proper policy and identification of crops that have low water requirements.

**Acknowledgements** Many thanks to Robert Horton, Professor of Soil Science, Iowa State University, for his guidance in preparing and conducting the research.

**Author contribution** All of the authors contributed to the study conception and design. Material preparation, data collection, and analysis were performed by Mehdi Asadi and Khalil Valizadeh Kamran. The first draft of the manuscript was written by Mehdi Asadi and all authors commented on the previous versions of the manuscript. All authors read and approved the final manuscript.

**Data availability** The datasets generated during and/or analyzed during the current study are available from the corresponding author on reasonable request.

## Declarations

**Conflict of interest** The authors declare no competing interests.

## References

- Alexandridis TK, Cherif I, Kalogeropoulos C, Monachou S, Eskridge K, Silleos N (2013) Rapid error assessment for quantitative estimations from Landsat 7 gap-filled images. *Rem Sens Lett* 4(9):920–928. <https://doi.org/10.1080/2150704X.2013.815380>
- Allen RG, Tasumi M, Morse A, Trezza R (2005) A Landsat-based energy balance and evapotranspiration model in Western US water rights regulation and planning. *Irrigat Drain Syst* 19(3–4):251–268. <https://doi.org/10.1007/s10795-005-5187-z>
- Allen RG, Tasumi M, Trezza R (2007) Satellite-based energy balance for mapping evapotranspiration with internalized calibration

- (METRIC)—Model. *J Irrigat Drain Eng* 133(4):380–394. [https://doi.org/10.1061/\(ASCE\)0733-9437\(2007\)133:4\(380\)](https://doi.org/10.1061/(ASCE)0733-9437(2007)133:4(380))
- Allen RG, Waters R, Tasumi M, Trezza R, Bastiaansen W (2002) SEBAL, surface energy balance algorithms for land Idaho implementation advanced training and user's manual, version 1.0: 90 p
- AlZayed IS, Elagib NA, Ribbe L, Heinrich J (2016) Satellite-based evapotranspiration over Gezira Irrigation Scheme, Sudan: a comparative study. *Agr Water Manag* 177:66–76. <https://doi.org/10.1016/j.agwat.2016.06.027>
- Asadi M, Karami M (2020) Estimation of evapotranspiration in Fars province using experimental indicators. *Journal of Applied Researches in Geographical Sciences* 20(S1):159–175
- Atasever UH, Ozkan C (2018) A new SEBAL approach modified with backtracking search algorithm for actual evapotranspiration mapping and on-site application. *J Indian Soci Rem Sens* 46(8):1213–1222. <https://doi.org/10.1007/s12524-018-0816-9>
- Bastiaanssen WG (2000) SEBAL-based sensible and latent heat fluxes in the irrigated Gediz Basin. *Turkey J Hydrol* 229(1–2):87–100. [https://doi.org/10.1016/S0022-1694\(99\)00202-4](https://doi.org/10.1016/S0022-1694(99)00202-4)
- Bastiaanssen WG, Menenti M, Feddes RA, Holtslag AA (1998) A remote sensing surface energy balance algorithm for land (SEBAL). *J Hydrol* 212–213:198–212. [https://doi.org/10.1016/S0022-1694\(98\)00253-4](https://doi.org/10.1016/S0022-1694(98)00253-4)
- Costa JDO, Coelho RD, Wolff W, José JV, Folegatti MV, Ferraz SF (2019) Spatial variability of coffee plant water consumption based on the SEBAL algorithm. *Scientia Agricola* 76(2):93–101. <https://doi.org/10.1590/1678-992x-2017-0158>
- Daughtry CST, Kustas WP, Moran MS, Pinter PJ, Jackson RD, Brown PW, Gay LW (1990) Spectral estimates of net radiation and soil heat flux. *Rem Sens Environ* 32(2–3):111–124. [https://doi.org/10.1016/0034-4257\(90\)90012-B](https://doi.org/10.1016/0034-4257(90)90012-B)
- Elnmer A, Khadr M, Kanae S, Tawfik A (2019) Mapping daily and seasonally evapotranspiration using remote sensing techniques over the Nile delta. *Agr Water Manag* 213:682–692. <https://doi.org/10.1016/j.agwat.2018.11.009>
- French AN, Hunsaker DJ, Bounoua L, Karnieli A, Luckett WE, Strand R (2018) Remote sensing of evapotranspiration over the central Arizona irrigation and drainage district, USA. *Agronomy* 8(12):278. <https://doi.org/10.3390/agronomy8120278>
- Genanu M, Alamirew T, Senay G, Gebremichael M (2017) Remote sensing based estimation of evapotranspiration using selected algorithms: the case of Wonji Shoa Sugar Cane Estate, Ethiopia: 2–14. <https://www.preprints.org/manuscript/201608.0098/v1>
- Horvat B (2013) Spatial dynamics of actual daily evapotranspiration. *Gradevinar*, 65(8): 693–705. <https://doi.org/10.14256/JCE.837.2013>
- Jacob F, Olioso A, Gu XF, Su Z, Seguin B (2002) Mapping surface fluxes using airborne visible, near infrared, thermal infrared remote sensing data and a spatialized surface energy balance model. *Agronomie* 22(6):669–680. <https://doi.org/10.1051/agro:2002053>
- Jovzi M, Zareabyaneh H, Hozhabr H, Khasraei A (2019) Estimate of potential evapotranspiration from energy balance method compared to evaporation pan and FAO Penman-Monteith methods. *Iranian Journal of Irrigation & Drainage* 13(3):727–736
- Khand K, Bhattarai N, Taghvaeian S, Wagle P, Gowda PH, Alderman PD (2021) Modeling evapotranspiration of winter wheat using contextual and pixel-based surface energy balance models. *Transactions of the ASABE* 64(2): 507–519. <https://doi.org/10.13031/trans.14087>
- Kundu S, Mondal A, Khare D, Hain C, Lakshmi V (2018) Projecting climate and land use change impacts on actual evapotranspiration for the Narmada river basin in central India in the future. *Rem Sens* 10(4):578. <https://doi.org/10.3390/rs10040578>
- Kustas WP, Daughtry CS (1990) Estimation of the soil heat flux/net radiation ratio from spectral data. *Agr Forest Meteorol* 49(3):205–223. [https://doi.org/10.1016/0168-1923\(90\)90033-3](https://doi.org/10.1016/0168-1923(90)90033-3)
- Kustas WP, Moran MS, Humes KS, Stannard DI, Pinter PJ, Hipps LE, Goodrich DC (1994) Surface energy balance estimates at local and regional scales using optical remote sensing from an aircraft platform and atmospheric data collected over semiarid rangelands. *Water Resour Res* 30(5):1241–1259. <https://doi.org/10.1029/93WR03038>
- Li H, Li ZY, Lei C, Li ZL, Shengwei Z (2008) Estimation of water consumption and crop water productivity of winter wheat in North China Plain using remote sensing technology. *Agr Water Manag* 95:1271–1278. <https://doi.org/10.1016/j.agwat.2008.05.003>
- Lian J, Huang M (2015) Evapotranspiration estimation for an oasis area in the Heihe River Basin using Landsat-8 images and the METRIC model. *Water Resour Manag* 29(14):5157–5170. <https://doi.org/10.1007/s11269-015-1110-z>
- Liou YA, Kar S (2014) Evapotranspiration estimation with remote sensing and various surface energy balance algorithms—a review. *Energies* 7(5):2821–2849. <https://doi.org/10.3390/en7052821>
- Losgedaragh SZ, Rahimzadegan M (2018) Evaluation of SEBS, SEBAL, and METRIC models in estimation of the evaporation from the freshwater lakes (case study: Amirkabir dam, Iran). *J Hydrol* 561:523–531. <https://doi.org/10.1016/j.jhydrol.2018.04.025>
- Ma W, Hafeez M, Rabbani U, Ishikawa H, Ma Y (2012) Retrieved actual ET using SEBS model from Landsat-5 TM data for irrigation area of Australia. *Atmos Environ* 59:408–414. <https://doi.org/10.1016/j.atmosenv.2012.05.040>
- Ma W, Hafeez M, Ishikawa H, Ma Y (2013) Evaluation of SEBS for estimation of actual evapotranspiration using ASTER satellite data for irrigation areas of Australia. *Theor Appl Climatol* 112(3–4):609–616. <https://doi.org/10.1007/s00704-012-0754-3>
- Mkhwanazi M, Chávez JL, Andales AA (2015) SEBAL-A: a remote sensing ET algorithm that accounts for advection with limited data. Part I: Development and validation. *Rem Sens* 7(11):15046–15067. <https://doi.org/10.3390/rs71115046>
- Moradi A, Babaei H, Alimohammadi A, Radiom S (2020) Estimation of crop coefficients in the Moghan cultivation industry and the study of relationship between evapotranspiration and yield performance. *Iranian Journal of Remote Sensing & GIS* 11(4): 11–28. <https://doi.org/10.52547/gisj.11.4.11>
- Nasrabadi I (2015) Environmental evidence of the Iranian water crisis and some solutions, social-cultural strategy quarterly. 4 (15): 65–89
- Oberg JW, Meless AM (2006) Evapotranspiration dynamics at an ecohydrological restoration site: an energy balance and remote sensing approach I. *J Am Water Resour Assoc* 42:565–582. <https://doi.org/10.1111/j.1752-1688.2006.tb04476.x>
- Owaneh OM, Suleiman AA (2018) Comparison of the Performance of ALARM and SEBAL in Estimating the Actual Daily ET from Satellite Data. *J Irrigat Drain Eng* 144(9):04018024. [https://doi.org/10.1061/\(ASCE\)IR.1943-4774.0001335](https://doi.org/10.1061/(ASCE)IR.1943-4774.0001335)
- Rahimpour M, Rahimzadegan M (2021) Assessment of surface energy balance algorithm for land and operational simplified surface energy balance algorithm over freshwater and saline water bodies in Urmia Lake Basin. *Theor Appl Climatol* 143(3):1457–1472. <https://doi.org/10.1007/s00704-020-03472-1>
- Rahimzadegan M, Janani A (2019) Estimating evapotranspiration of pistachio crop based on SEBAL algorithm using Landsat 8 satellite imagery. *Agr Water Manag* 217:383–390. <https://doi.org/10.1016/j.agwat.2019.03.018>
- Rawat KS, Bala A, Singh SK, Pal RK (2017) Quantification of wheat crop evapotranspiration and mapping: a case study from Bhiwani

- District of Haryana, India. *Agr Water Manag* 187:200–209. <https://doi.org/10.1016/j.agwat.2017.03.015>
- Ruhoff AL, Paz AR, Collischonn W, Aragao LE, Rocha HR, Malhi YS (2012) A Modis-based energy balance to estimate evapotranspiration for clear-sky days Brazilian tropical savannas. *Rem Sens* 4:703–725. <https://doi.org/10.3390/rs4030703>
- Singh RK, Irmak A, Irmak S, Martin DL (2008) Application of SEBAL model for mapping evapotranspiration and estimating surface energy fluxes in south-central Nebraska. *J Irrigat Drain Eng* 134(3):273–285. [https://doi.org/10.1061/\(ASCE\)0733-9437\(2008\)134:3\(273\)](https://doi.org/10.1061/(ASCE)0733-9437(2008)134:3(273))
- Su Z (2002) The Surface Energy Balance System (SEBS) for estimation of turbulent heat fluxes. *Hydrol Earth Syst Sci* 6(1):85–100. <https://doi.org/10.5194/hess-6-85-2002>
- Suleiman A, Al-Bakri J (2011) Estimating actual evapotranspiration using ALARM and the dimensionless temperature, Evapotranspiration. InTech Publisher, Croatia, pp 163–194
- Suleiman A, Crago R (2002a) Analytical land–atmosphere radiometer model. *J Appl Meteorol* 41(2):177–187. [https://doi.org/10.1016/S0168-1923\(02\)00127-2](https://doi.org/10.1016/S0168-1923(02)00127-2)
- Suleiman A, Crago R (2002b) Analytical land–atmosphere radiometer model. *Agr Forest Meteorol* 41:177–187. [https://doi.org/10.1175/1520-0450\(2002\)041%3c0177:ALARM%3e2.0.CO;2](https://doi.org/10.1175/1520-0450(2002)041%3c0177:ALARM%3e2.0.CO;2)
- Suleiman A, Crago R (2004) Hourly and daytime evapotranspiration from grassland using radiometric surface temperatures. *Agron J* 96(2):384–390. <https://doi.org/10.2134/agronj2004.3840>
- Suleiman A, Al-Bakri J, Duqqah M, Crago R (2008) Intercomparison of evapotranspiration estimates at the different ecological zones in Jordan. *J Hydrometeorol* 9(5):903–919. <https://doi.org/10.1175/2008JHM920.1>
- Suleiman AA, Al-Bakri JT, Duqqah M (2007) A comparison study of MODIS and ASCE alfalfa evapotranspiration in a semiarid climate. In 2007 ASAE Annual Meeting (p. 1). American Society of Agricultural and Biological Engineers
- Widyantara AP, Solihuddin T (2020) Pemetaan Perubahan Luasan Lahan Mangrove di Pesisir Probolinggo Menggunakan Citra Satelit. *Jurnal Penginderaan Jauh dan Pengolahan Data Citra Digital* 17(2): 75–87. <http://repository.lapan.go.id/id/eprint/968>.
- Zhou X, Bi S, Yang Y, Tian F, Ren D (2014) Comparison of ET estimations by the three-temperature model, SEBAL model and eddy covariance observations. *J Hydrol* 519:769–776. <https://doi.org/10.1016/j.jhydrol.2014.08.004>
- Zoratipour E, Soltani A, Zoratipour A (2019) Spatial and temporal evaluation of different methods for prediction of reference evapotranspiration (case study: Khuzestan province). *Iran J Ecohydrol* 6(2): 465–478. <https://doi.org/10.22059/ije.2019.272676.1017>

**Publisher's Note** Springer Nature remains neutral with regard to jurisdictional claims in published maps and institutional affiliations.